

The Crystal Structure and Bonding of Fluor-Tremolite: a Comparison with Hydroxyl Tremolite

MARYELLEN CAMERON, AND G. V. GIBBS

*Department of Geological Sciences,
Virginia Polytechnic Institute and State University,
Blacksburg, Virginia 24061*

Abstract

The crystal structure of synthetic fluor-tremolite [$a = 9.787(3)\text{\AA}$, $b = 18.004(2)\text{\AA}$, $c = 5.263(2)\text{\AA}$, $\beta = 104.44(2)^\circ$, $C2/m$] has been refined and compared with that of hydroxyl tremolite. Examination of the structures reveals that substitution of F for OH significantly reduces the size of the octahedral layer and, accordingly, the a and b cell parameters. The double chains of tetrahedra in the two structures are very similar, and the small differences within the individual tetrahedra can be explained in terms of differences in the octahedral layers. The $T(2)$ -tetrahedra in both hydroxyl and fluor-tremolite are larger (1.632\AA and 1.629\AA , respectively) and more distorted than the $T(1)$ -tetrahedra (both 1.620\AA).

The higher thermal stability of fluor-tremolite may be attributed in part to the stronger Mg–F bonds, and in part to instability created by excessive charge imbalance in the structure during the dehydroxylation of hydroxyl tremolite.

Introduction

For compositions so far investigated, the replacement of OH by F significantly raises the upper thermal stability limit of an amphibole. Troll and Gilbert (1972) have shown, for example, that the upper limit at 1 atm of fluor-tremolite is $\sim 1150^\circ\text{C}$ which is more than 600°C higher than that of hydroxyl tremolite ($\sim 525^\circ\text{C}$ at 1 atm, extrapolated from Boyd, 1959). This result indicates that the replacement of OH by F should be of petrologic importance because fluorine bearing amphiboles will be stable in high temperature igneous environments where pure hydroxyl amphiboles might otherwise be unstable. Fe-rich sodic amphiboles are common in peralkaline rhyolites and trachytes, rocks which apparently crystallize at high temperatures. However, Ernst (1962) demonstrated that hydroxyl Fe-rich sodic amphiboles should not occur as primary phases in rocks crystallizing at such high temperatures. Citing the work of Comeforo and Kohn (1954), he suggests that the presence of fluorine may have stabilized these amphiboles.

Since the replacement of OH by F plays a significant role in dictating the upper thermal stability of an amphibole, comparison of the crystal structures of hydroxyl and fluor-tremolite may reveal differences which could provide clues to understanding their

differing thermal stabilities. In addition, the study should clarify the steric effects induced in the clin amphibole structure as a result of substituting F for OH. Correlations between selected bond lengths and Mulliken bond overlap populations will also be presented. Tremolites were selected for study for the following reasons: (1) a careful and precise refinement of the hydroxyl tremolite crystal structure has recently been published (Papike, Ross, and Clark, 1969), (2) fluor-tremolite crystals large enough for single crystal work can be synthesized with little difficulty, and (3) the complications arising from interactions between the OH and F and an A site cation are avoided because the cation is absent.

Experimental Procedures

The fluor-tremolite crystals used in our study were synthesized from an oxide mix having the bulk composition $[\text{CaCO}_3 \cdot \text{CaF}_2 \cdot 5\text{MgO} \cdot 8\text{SiO}_2]$. The mix was placed in a drying furnace for one hour at 1000°C to drive off the CO_2 in the calcium carbonate and then sealed in platinum capsules. The resultant charges were heated to 1150°C in a platinum-wound quenching furnace and maintained at this temperature for one week. The charges were converted to greater than 95 percent fluor-tremolite crystals whose size varied up to 0.8 mm.

The crystal selected for the X-ray study was approximately $0.1 \times 0.1 \times 0.08$ mm. Its unit cell parameters, calculated from data collected along $[100]^*$, $[010]^*$ and $[001]^*$ with a Picker four-circle, single-crystal diffractometer, are compared (Table 1) with those of a natural, relatively pure hydroxyl tremolite. Diffractometer settings were calculated with C. T. Prewitt's GSET 4 computer program, and about 1200 intensity data were automatically collected using Nb-filtered Mo radiation. The data were reduced using a program written by Prewitt, and reflections with structural amplitudes less than four times their estimated standard deviations were removed prior to the refinement. No corrections were made for primary and secondary extinction or for absorption effects ($\mu = 13.5 \text{ cm}^{-1}$). An isotropic least-squares refinement of the fluor-tremolite structure in space group $C2/m$ was calculated using the structural data of hydroxyl tremolite (Papike, 1969) as starting parameters, neutral atom scattering factors (Doyle and Turner, 1968) and the ORFL programs (Busing, Martin, and Levy, 1962). It was assumed that the $M(1)$ -, $M(2)$ - and $M(3)$ -octahedra are completely occupied by magnesium, the $M(4)$ -“tetragonal antiprism” by calcium, the $T(1)$ - and $T(2)$ -tetrahedra by silicon, and that the A site is vacant. Unit weights were used in the initial stages of the refinement, but after convergence the structural amplitudes were weighted according to a scheme devised by Hanson (1965) which gives less weight to the relatively inaccurate weak reflections and to the strong ones which are often affected by extinction. The weight for each $|F_{\text{obs}}|$ is given by

$$w = \frac{1}{\sigma^2 |F_{\text{obs}}|} = \frac{1}{\{1 + [(|F_{\text{obs}}| - \text{PA} \cdot F_t) / \text{XX} \cdot F_t]^2\}^{1/2}}$$

where F_t is the minimum $|F_{\text{obs}}|$ used in the refinement. The constants (PA and XX) in the equation were adjusted until constant $\langle w\Delta^2 \rangle$ for groups of increasing $|F_{\text{obs}}|$ was achieved, thereby making the weights essentially independent of the magnitude of $|F_{\text{obs}}|$. Observed and calculated structure amplitudes are listed in Table 2.

The final parameters from the isotropic refinement were used as starting ones for an anisotropic refinement of the structure. The R -factor ratio test of Hamilton (1965) revealed that the anisotropic thermal model yielded a significantly better R -factor than did the isotropic model. The final R -factor was

TABLE 1. Crystal Data*

	Hydroxyl tremolite (Papike et al., 1969)	Fluor-tremolite
a	9.818(5) Å	9.787(3) Å
b	18.047(8)	18.004(2)
c	5.275(3)	5.263(2)
β	104.65°(5)	104.44°(2)
Cell volume	904.2(6) Å ³	898.1(5) Å ³
Space group	$C2/m$	$C2/m$
Calculated density	2.99 g/cc	3.019 g/cc
Crystal size	0.31×0.15×0.22 mm	0.1×0.1×0.08 mm
μ	14.4 cm ⁻¹	13.5 cm ⁻¹
Number of $ F_0 $'s	1701 $ F_0 > 0$	865 $ F_0 > 4\sigma$
Final R -factor	0.035	0.042

* Estimated standard deviations are given in parentheses and refer to last digit quoted.

0.042. Anisotropic temperature factor coefficients are given in Table 3. Positional parameters determined from the refinement of the fluor-tremolite (Table 4) were used in Busing, Martin and Levy's (1964) ORFFE program to calculate interatomic distances, angles (Table 5), and magnitudes, orientations and the associated estimated standard deviations of the apparent thermal ellipsoids (Table 6). All of the thermal ellipsoids for atoms in fluor-tremolite are triaxial, although most tend toward ellipsoids of revolution. The rms displacements range from 0.05 Å for silicon to 0.12 Å for O(7) and Ca, and are slightly larger than those of corresponding atoms in hydroxyl tremolite. Atoms in the O(5), O(6) and $M(4)$ sites have the most anisotropic ellipsoids.

Bond overlap populations were calculated using an extended Hückel molecular orbital program originally written by Hoffmann (1963). The diagonal elements H_{ii} of the Hamiltonian matrix are approximated by the negative of the valence state ionization potentials (VSIP) whereas the off-diagonal elements H_{ij} are approximated by the Wolfsberg-Helmholz parametrization (1952)

$$H_{ij} = S_{ij}(H_{ii} + H_{jj})$$

where S_{ij} is the overlap integral between the i th and j th atomic orbitals (see Louisnathan and Gibbs, 1972) of two atoms in a coordination anion.

Only the $3s$ and $3p$ valence orbitals of silicon and the $2s$ and $2p$ of oxygen were used in the calculations. Input to the program consisted of the atom coordinates, the VSIP values of Basch, Viste, and Gray (1965) and the free-atom orbital exponents of Clementi and Raimondi (1963).

TABLE 2. Observed and Calculated Structure Amplitudes for Fluor-Tremolite*

Table with 14 columns: h, k, l, F(obs), F(calc), h, k, l, F(obs), F(calc), h, k, l, F(obs), F(calc), h, k, l, F(obs), F(calc). The table contains multiple rows of numerical data representing structure amplitudes for various hkl reflections.

TABLE 3. Anisotropic Temperature Factor Coefficients ($\times 10^5$)^{*}

Atom	β_{11}	β_{22}	β_{33}	β_{12}	β_{13}	β_{23}
O(1)	118(30)	38(11)	501(120)	9(13)	9(50)	1(25)
O(2)	210(32)	49(11)	382(108)	-1(14)	95(50)	-18(26)
O(3)	122(36)	71(14)	580(136)	0	88(58)	0
O(4)	167(33)	42(10)	570(116)	-22(13)	48(51)	-28(27)
O(5)	194(29)	40(10)	570(10)	12(13)	40(44)	72(26)
O(6)	98(27)	74(10)	420(103)	24(14)	3(44)	-4(27)
O(7)	226(45)	70(16)	884(171)	0	234(73)	0
M(1)	94(21)	42(8)	309(78)	0	-18(34)	0
M(2)	197(22)	40(8)	408(78)	0	101(35)	0
M(3)	105(30)	24(10)	489(112)	0	19(49)	0
M(4)	249(13)	66(4)	680(45)	0	262(21)	0
T(1)	87(11)	26(4)	257(40)	-6(5)	71(18)	10(10)
T(2)	85(11)	37(4)	206(39)	-5(5)	-7(18)	11(10)

* Estimated standard deviations are given in parentheses and refer to the last digit.

The general structure of clin amphiboles is well known (Warren, 1929; Zussman, 1959) and the reader is referred to Papike *et al* (1969) for details. Figure 1 shows the structure of tremolite projected down *c* with the nomenclature of the atoms given in the upper left corner and the *z* fractional coordinates in the upper right.

Discussion

Using extended Hückel molecular orbital (EHMO) theory, Gibbs, Hamil, Louisnathan, Bartell, and Yow

TABLE 4. Positional and Isotropic Temperature Factors^{*}

Atom	Parameter	Fluor-tremolite	Atom	Parameter	Fluor-tremolite
O(1)	x	0.1126(3)	M(1)	x	0
	y	0.0847(2)		y	0.0885(1)
	z	0.2179(6)		z	0.5
	B	0.49(5)		B	0.40(4)
O(2)	x	0.1187(3)	M(2)	x	0
	y	0.1702(2)		y	0.1760(1)
	z	0.7239(6)		z	0
	B	0.55(5)		B	0.51(4)
O(3)	x	0.1020(4)	M(3)	x	0
	y	0		y	0
	z	0.7124(8)		z	0
	B	0.60(6)		B	0.37(5)
O(4)	x	0.3644(4)	M(4)	x	0
	y	0.2484(2)		y	0.2771(1)
	z	0.7907(7)		z	0.5
	B	0.62(6)		B	0.73(2)
O(5)	x	0.3471(3)	T(1)	x	0.2829(1)
	y	0.1351(2)		y	0.0834(1)
	z	0.1001(7)		z	0.2960(2)
	B	0.62(5)		B	0.29(2)
O(6)	x	0.3444(3)	T(2)	x	0.2900(1)
	y	0.1197(2)		y	0.1707(1)
	z	0.5857(6)		z	0.8041(2)
	B	0.52(5)		B	0.31(2)
O(7)	x	0.3408(5)			
	y	0			
	z	0.2922(10)			
	B	0.71(8)			

* Estimated standard deviations are given in parentheses and refer to the last digit.

(1972), Louisnathan and Gibbs (1972) and Gibbs, Louisnathan, Ribbe, and Phillips (1973) have shown that Si-O bond overlap populations, $n(\text{Si-O})$, are inversely correlated with observed Si-O bond lengths for a number of silicates. As no amphiboles were included in these studies, similar calculations were made for hydroxyl and fluor-tremolite (Table 7). Although EHMO calculations are usually made using observed bond angles and constant bond lengths,¹ this proved to be impracticable in the case of the amphibole chains and so $n(\text{Si-O})$ for the two tremolites were calculated using observed O-Si-O and Si-O-Si angles and Si-O distances. However, since observed Si-O bond lengths correlate with (1) $n(\text{Si-O})$ calculated using observed angles and constant distance and (2) $n(\text{Si-O})$ calculated using both observed angles and distances, it is apparent that a correlation must exist between (1) and (2). This is evinced by Figure 2 which was constructed from the data of Gibbs *et al* (1972). The fact that the trend between (1) and (2) is well-developed ($r = 0.95$) indicates that the bond overlap populations derived from EHMO calculations using observed bond lengths should be valid in rationalizing the Si-O bond length variation in the two amphiboles.

For the two tremolites, the bond overlap populations calculated for the underbonded oxygens are greater than those calculated for the overbonded ones and may reflect in part the balancing of valences on the oxygens. Figure 3 shows a plot of $\Delta\zeta(\text{O})$, which is a measure of the underbonded or overbonded nature of an oxygen anion (Baur, 1970), *vs* $n(\text{Si-O})$. A similar trend is obtained by plotting $\Delta\zeta(\text{O})$ *vs* $n(\text{Si-O})$ for silicates (Gibbs *et al*, 1972), in which the tetrahedral bond overlap populations were calculated using constant bond lengths (Fig. 4). Although Baur's work is based on electrostatic considerations and the EHMO model on covalent considerations, the two apparently are not incongruous (Pauling, 1961). In fact, Pant and Cruickshank (1967, p. 293) have stated that "we should expect a balancing of the valences whether the bonds are ionic or covalent or a mixture." Thus the shortening of bonds to underbonded oxygens may be explained in part in terms of the increased Si-O bond overlap

¹ Constant bond lengths are utilized because short bonds with large overlap integrals would tend to have larger overlap populations than long bonds if observed bond lengths are used in the EHMO calculations (Bartell *et al*, 1970).

population which is required for charge balance of the oxygens. However, not all the shortening can be rationalized in this fashion as the non-tetrahedral cations certainly play an important role in dictating Si-O bond length variations (Smith, 1954; Baur, 1961, 1970).

T(1)- and T(2)-tetrahedra

The mean T-O bond length for the *T(1)*-tetrahedron is identical (1.620Å) in both hydroxyl and fluor-tremolite. *T(1)*-O(1) is the shortest interatomic distance in the double chains in both amphiboles and may reflect the larger overlap populations for the bonds to the non-bridging oxygens. The significantly longer *T(1)*-O(1) distance in fluor-tremolite may be explained as a necessary geo-

TABLE 5. Interatomic Distances (Å) and Angles (Degrees) in Hydroxyl and Fluor-Tremolite*

Atoms	Hydroxyl tremolite**		Fluor-tremolite	
	distance	angle at metal atom	distance	angle at metal atom
T(1)-O(1)	1.602(2)		1.614(3)	
-O(5)	1.632(2)		1.628(3)	
-O(6)	1.629(2)		1.630(4)	
-O(7)	1.616(1)		1.606(2)	
mean	1.620		1.620	
O(1)-O(5)	2.681(3)	111.9(1)	2.680(4)	111.6(2)
-O(6)	2.666(3)	111.1(1)	2.664(5)	110.4(2)
-O(7)	2.649(2)	110.7(1)	2.651(5)	110.8(2)
O(5)-O(6) ^{†P}	2.602(3)	105.8(1)	2.578(5)	104.6(2)
-O(7)	2.638(2)	108.5(1)	2.641(4)	109.5(2)
O(6)-O(7)	2.639(2)	108.7(1)	2.647(4)	109.7(2)
mean	2.646	109.4	2.644	109.4
T(2)-O(2)	1.616(2)		1.623(3)	
-O(4)	1.586(2)		1.587(3)	
-O(5)	1.653(2)		1.648(4)	
-O(6)	1.672(2)		1.659(3)	
mean	1.632		1.629	
O(2)-O(4)	2.736(2)	117.3(1)	2.732(4)	116.7(2)
-O(5)	2.670(3)	109.4(1)	2.666(5)	109.2(2)
-O(6)	2.665(3)	108.2(1)	2.652(4)	107.8(2)
O(4)-O(5)	2.645(2)	109.4(1)	2.642(4)	109.5(2)
-O(6) ^{†P}	2.560(2)	103.5(1)	2.543(4)	103.1(2)
O(5)-O(6)	2.702(3)	108.6(1)	2.715(5)	110.3(2)
mean	2.663	109.4	2.658	109.4
T(1)-T(1) across mirror	3.030(2)		3.002(2)	
-T(2) through O(5)	3.051(2)		3.045(2)	
-T(2) through O(6)	3.086(2)		3.088(2)	
T(1)-O(7)-T(1)	139.3(2)		138.3(3)	
T(1)-O(5)-T(2)	136.5(1)		136.7(2)	
T(1)-O(6)-T(2)	138.4(1)		139.7(2)	
O(5)-O(6)-O(5)	167.6(1)		167.9(2)	
M(1)-O(1)	[2] ^{††} 2.064(2)		2.059(3)	
-O(2)	[2] 2.078(2)		2.054(4)	
-O(3)	[2] 2.083(2)		2.057(3)	
mean	2.075		2.057	

* Estimated standard deviations are given in parentheses and refer to the last digit.

** Papike et al., 1969.

^{†P} Edge shared between tetrahedron and M(4) polyhedron.

^{††} Multiplicity of bond.

^{∞∞} Edge shared between two octahedra.

^{OP} Edge shared between octahedron and M(4) polyhedron.

TABLE 5, Continued

Atoms	Hydroxyl tremolite**		Fluor-tremolite	
	distance	angle at metal atom	distance	angle at metal atom
O(1)-O(2)	[2]	95.68(7)	3.064(5)	96.3(1)
-O(2) ^{∞∞}	[2]	85.63(7)	2.818(4)	86.5(1)
-O(3)	[2]	94.96(9)	3.040(5)	95.2(1)
-O(3) ^{∞∞}	[2]	83.66(9)	2.694(4)	81.8(1)
O(2)-O(3)	[2]	95.91(7)	3.069(3)	96.6(1)
-O(2) ^{OP}	[1]	87.23(8)	2.867(6)	88.5(2)
O(3)-O(3) ^{∞∞}	[1]	80.96(8)	2.600(7)	78.4(2)
mean		89.99	2.903	90.0
M(2)-O(1)	[2]	2.133(2)	2.146(4)	
-O(2)	[2]	2.083(2)	2.077(3)	
-O(4)	[2]	2.014(2)	2.024(4)	
mean	2.077		2.082	
O(1)-O(1)	[1]	79.95(7)	2.757(6)	80.0(2)
-O(2)	[2]	92.11(7)	3.036(5)	91.9(1)
-O(2) ^{∞∞}	[2]	83.74(7)	2.818(4)	83.7(1)
-O(4)	[2]	92.83(6)	3.015(4)	92.6(1)
O(2)-O(4)	[2]	93.40(7)	2.984(5)	93.3(1)
-O(4) ^{OP}	[2]	90.25(8)	2.914(5)	90.5(1)
O(4)-O(4)	[1]	95.00(8)	2.997(7)	95.5(2)
mean		89.97	2.941	90.0
M(3)-O(1)	[4]	2.070(2)	2.055(3)	
-O(3)	[2]	2.057(3)	2.011(4)	
mean	2.066		2.040	
O(1)-O(1)	[2]	97.09(6)	3.049(6)	95.8(2)
-O(1) ^{∞∞}	[2]	82.91(7)	2.757(6)	84.2(2)
-O(3)	[4]	95.86(6)	3.040(5)	97.0(1)
-O(3) ^{∞∞}	[4]	84.14(6)	2.694(4)	83.0(1)
mean		90.00	2.879	90.0
M(4)-O(2)	[2]	2.397(2)	2.400(4)	
-O(4)	[2]	2.321(2)	2.308(3)	
-O(5)	[2]	2.767(2)	2.756(3)	
-O(6)	[2]	2.539(2)	2.514(3)	
mean	2.506		2.459	
O(2)-O(4)	[2]		3.119(5)	83.0(1)
-O(5)	[2]		3.619(5)	88.9(1)
O(6)-O(4) ^{†P}	[2]		2.543(4)	63.5(1)
-O(5) ^{†P}	[2]		2.578(5)	58.4(1)
O(4)-O(2) ^{OP}	[2]		2.984(5)	78.6(1)
-O(5)	[2]		3.414(5)	84.3(1)
O(6)-O(5)	[2]		3.072(3)	71.2(1)
-O(6)	[1]		3.386(6)	84.7(1)
O(2)-O(2) ^{OP}	[1]		2.867(6)	73.4(2)
mean			3.057	
M(1)-M(1)		3.169(2)	3.187(4)	
-M(2)		3.086(2)	3.067(2)	
-M(3)		3.077(1)	3.076(1)	
-M(4)		3.423(2)	3.395(3)	
M(2)-M(3)		3.187(2)	3.168(2)	
M(2)-M(4)		3.204(1)	3.200(2)	

metrical adjustment of the structure to accommodate the smaller *M(1)*-octahedron.

The O(nbr)-T-O(br) angles in the *T(1)*-tetrahedron of both tremolites are larger than the O(br)-T-O(br) angles as predicted and discussed by Gibbs (1969). One of the O(br)-T-O(br) angles, O(5)-T-O(6), is much smaller than either of the other two angles of this type. This is apparently due to the fact that the O(5)-O(6) tetrahedral edge is shared with the *M(4)*-"tetragonal antiprism." This sharing produces cation-cation repulsion across the shared edge and results in a shortening of the O(5)-O(6)

TABLE 6. Magnitudes and Orientations of the Principal Axes of the Thermal Ellipsoids*

Atom	Ellipsoid axis	rms displacement	Angles, with respect to		
			a	b	c
O(1)	1	.068(11)	41(20)	111(36)	69(24)
	2	.080(11)	95(45)	152(37)	115(42)
	3	.089(8)	49(20)	73(43)	147(37)
O(2)	1	.067(10)	103(14)	76(19)	14(18)
	2	.090(10)	96(49)	166(20)	76(18)
	3	.098(7)	15(23)	92(48)	90(18)
O(3)	1	.072(12)	6(31)	90	111(31)
	2	.088(10)	96(31)	90	159(31)
	3	.108(10)	90	90	90
O(4)	1	.070(11)	60(16)	44(17)	69(19)
	2	.091(9)	116(64)	106(52)	20(19)
	3	.096(8)	139(54)	50(33)	89(74)
O(5)	1	.060(12)	97(11)	42(10)	128(10)
	2	.096(7)	154(44)	112(29)	90(37)
	3	.103(7)	115(45)	55(23)	38(10)
O(6)	1	.060(11)	36(20)	101(8)	70(22)
	2	.080(9)	122(22)	78(11)	22(21)
	3	.113(8)	74(8)	17(9)	98(10)
O(7)	1	.083(13)	32(14)	90	136(14)
	2	.107(12)	90	180	90
	3	.116(10)	58(14)	90	46(14)
M(1)	1	.055(9)	54(14)	90	50(14)
	2	.078(7)	144(14)	90	40(14)
	3	.084(8)	90	0	90
M(2)	1	.071(7)	108(12)	90	3(12)
	2	.081(8)	90	180	90
	3	.095(5)	18(12)	90	87(12)
M(3)	1	.063(14)	90	0	90
	2	.068(10)	148(25)	90	107(25)
	3	.085(9)	58(25)	90	163(25)
M(4)	1	.069(4)	46(3)	90	151(3)
	2	.104(3)	90	180	90
	3	.116(3)	44(3)	90	61(3)
T(1)	1	.047(6)	49(10)	68(11)	143(11)
	2	.065(4)	121(40)	115(54)	126(12)
	3	.069(4)	124(38)	34(46)	87(36)
T(2)	1	.048(6)	68(10)	94(7)	36(10)
	2	.067(4)	149(12)	114(13)	59(11)
	3	.080(4)	111(12)	24(13)	73(9)

* Estimated standard deviations are given in parentheses and refer to the last digit.

distance with an accompanying decrease in the angle opposite this edge.

The $T(2)$ -tetrahedra in both structures are also statistically identical in size ($\sim 1.630\text{\AA}$), but they are larger and more distorted than the $T(1)$ -tetrahedra. The $T(2)$ -O(2)nbr distance in fluor-tremolite is only slightly longer than that in hydroxyl tremolite, which again may be the result of articulation requirements between the tetrahedral and octahedral layers. In fluor-tremolite, the $M(2)$ -octahedron is the only one of the four polyhedra in the octahedral layer which does not contract when fluorine is substituted for OH in the O(3) position. Thus, geometry does not dictate a lengthening of the $T(2)$ -O(2) interatomic distance, as was the case with $T(1)$ -O(1), in order to achieve simultaneous coordination in the octahedral layer.

The $T(2)$ -tetrahedron contains two non-bridging oxygens, O(2) and O(4), and two bridging oxygens, O(5) and O(6); the O(4) is highly underbonded, the O(2) only slightly so, and O(5) and O(6) are overbonded. If variable bond overlap populations can be used as a mechanism for balancing the charges on oxygens, we would expect the bond overlap populations to be significantly larger for the $T(2)$ -O(4) bond than for the $T(2)$ -O(2) and the $n(\text{Si-O})$ for both of these bonds to be larger than those for O(5) and O(6). This is the situation in both tremolites. The relative magnitudes of the Si-O bond overlap populations and the highly underbonded nature of O(4) may serve to explain in part why the $T(2)$ -O(4) bond is significantly shorter than the other tetrahedral bonds.

Since the O(2)- $T(2)$ -O(4) angle is the only O(nbr)- T -O(nbr) angle in either of the amphibole tetrahedra, it is the widest angle, as expected. The O(2)- $T(2)$ -O(5) and O(2)- $T(2)$ -O(6) angles are of intermediate size and the tetrahedral angles involving the bridging oxygens are the narrowest. The O(4)- $T(2)$ -O(6) angle is smaller than the other angles between the basal oxygens because it is opposite the O(4)-O(6) edge which is shared between the tetrahedron and the $M(4)$ -polyhedron.

The tetrahedral chains in hydroxyl and fluor-tremolite are very similar. Not only are the sizes of the $T(1)$ - and $T(2)$ -tetrahedra statistically identical, but the O(5)-O(6)-O(5) angle in fluor-tremolite is only slightly smaller than that in hydroxyl tremolite, indicating that the ditrigonal character of the rings in the tetrahedral chains is also similar in the two structures.

Octahedral layer

The most conspicuous difference between the octahedral layer of hydroxyl tremolite and fluor-tremolite is the smaller size of the $M(3)$ -, $M(1)$ - and $M(4)$ -octahedra in fluor-tremolite (2.040 \AA , 2.057 \AA , 2.495 \AA , respectively) as compared with those in hydroxyl-tremolite (2.066 \AA , 2.075 \AA , 2.506 \AA , respectively). The thinner octahedral layer in fluor-tremolite is reflected in its smaller a and b cell dimensions (Table 1). The size of the $M(2)$ -octahedron, which has 6 oxygen ligands, is identical in both tremolites; a comparison of bond angles also reveals no significant differences between the two $M(2)$ -octahedra. Thus the $M(2)$ -octahedron acts as a rigid unit in the octahedral layer and has not distorted in any manner in response to the decrease

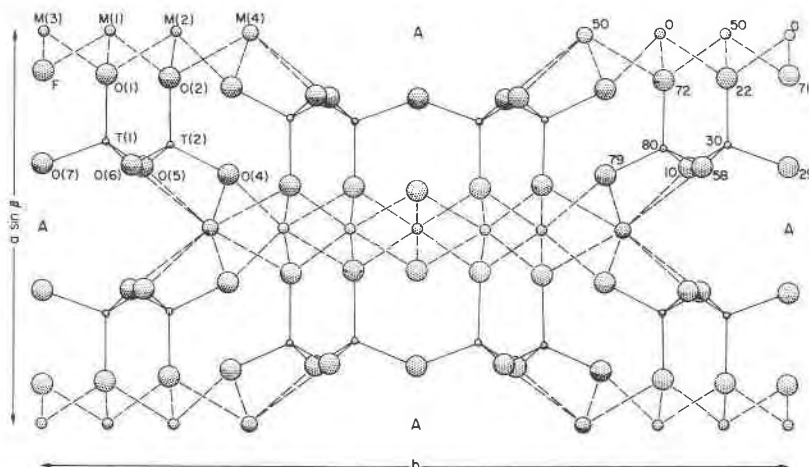


FIG. 1. The structure of tremolite projected down c . The nomenclature of the atoms is given in the upper left corner and the z fractional coordinates in the upper right. The vacant A site is indicated in this figure by the letter A .

in size of the other polyhedra in the octahedral layer. This is borne out by the mean quadratic elongation parameter, a distortion index proposed by Robinson, Gibbs, and Ribbe (1971) which calculates the same for the $M(2)$ -octahedron in both structures (Table 8).

The difference in size between the $M(1)$ - and $M(3)$ -octahedra in the two tremolites can be explained by the fact that three-coordinated hydroxyl ($r = 1.34\text{\AA}$; Ribbe and Gibbs, 1971) is larger than three-coordinated fluorine ($r = 1.30\text{\AA}$). A comparison of the $F\text{-Mg}$ and OH-Mg distances reveals that the effective radius of fluorine is 0.036\AA less than OH . The attending decrease in the Mg-O bonds in the octahedra which have fluorine ligands is apparently an effect related to the fluorine. EHM0 calculations for both octahedra using [4 oxygens and 2 OH ligands] and [4 oxygens and 2F ligands] with identical geometry revealed that the $n(\text{Mg-O})$ overlap

populations are greater for the latter case, thus possibly explaining the shorter Mg-O distances in fluor-tremolite.

Since the polyhedra in the octahedral layer share edges, it can be expected that cation-cation repulsion across shared edges will displace the Mg -cations from the centers of their octahedra. The displacement of the cations is toward the periphery of the octahedral layer, and the effect is most evident for the Mg cation in the $M(2)$ -octahedron in both structures. The displacement of Mg in the $M(1)$ -octahedron from the center of the octahedron is less than that for the $M(2)$ -octahedron and is approximately twice as large in fluor-tremolite as in hydroxyl tremolite.

TABLE 7. Bond Overlap Populations for Hydroxyl and Fluor-Tremolite Calculated Using Extended Hückel Molecular Orbital Theory

Bond	$n(\text{Si-O}_{\text{obs}})$	
	Hydroxyl tremolite	Fluor-tremolite
T(1)-O(1)	0.527	0.519
T(1)-O(5)	.487	.490
T(1)-O(6)	.491	.490
T(1)-O(7)	.500	.506
T(2)-O(2)	.523	.516
T(2)-O(4)	.534	.532
T(2)-O(5)	.478	.483
T(2)-O(6)	.459	.468

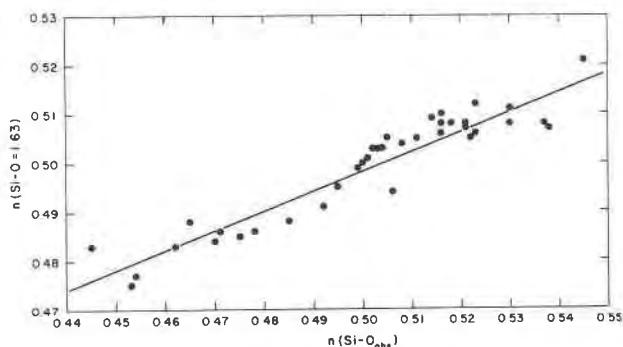


FIG. 2. Variation of $n(\text{Si-O} = 1.63)$ with $n(\text{Si-O}_{\text{obs}})$ for nine silicates using data from Gibbs *et al* (1971). [$n(\text{Si-O} = 1.63)$ is calculated using constant bond lengths of 1.63\AA and $n(\text{Si-O}_{\text{obs}})$ is calculated using observed bond lengths.] The $n(\text{Si-O})$ values were calculated assuming constant Si-O bond lengths, observed O-Si-O angles, and s - and p -basis functions.

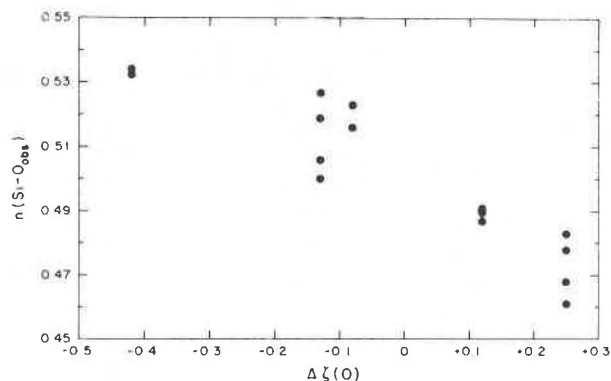


FIG. 3. Variation of $n(\text{Si}-\text{O}_{\text{obs}})$ with $\Delta\zeta(\text{O})$ for hydroxyl and fluor-tremolite. $\Delta\zeta(\text{O}) = \zeta(\text{O}) - \langle\zeta(\text{O})\rangle$ where $\zeta(\text{O})$ is the sum of Pauling bond strengths received by oxygen and $\langle\zeta(\text{O})\rangle$ is the mean $\zeta(\text{O})$ in a given tetrahedron.

In the repulsion process, shared edges are shortened and the angle opposite them becomes narrower. An examination of Table 5 shows that this is true for all shared polyhedral edges in the tremolites. The difference in the $\text{O}(3)-\text{M}(1)-\text{O}(3)$ angle in the two structures (78.4° in fluor-tremolite, 81.0° in hydroxyl tremolite) reflects the difference in length of the $\text{O}(3)-\text{O}(3)$ shared edge which results from the greater displacement of Mg and the weaker antibonding repulsions between adjacent fluorines in the fluor-tremolite. The angle $\text{O}(1)-\text{M}(2)-\text{O}(1)$ is identical in both structures as expected since the displacement of the $\text{M}(2)$ cation along b towards the edge of the octahedral layer is the same in both hydroxyl and fluor-tremolite.

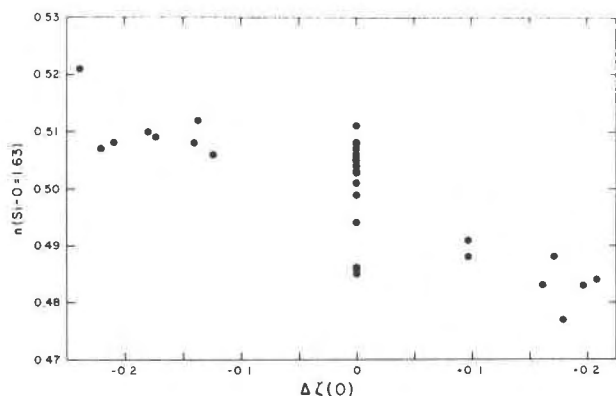


FIG. 4. Variation of $n(\text{Si}-\text{O} = 1.63)$ with $\Delta\zeta(\text{O})$ for nine silicates using the data from Gibbs *et al* (1971). The spread in bond overlap populations at $\Delta\zeta(\text{O}) = 0$ is the result of spread in $\text{Si}-\text{O}-\text{Si}$ angles (134° to 180°) which is not taken into account in the calculation of $\Delta\zeta(\text{O})$.

Structural environment of O(3)

The O(3) site in amphiboles lies in the mirror plane parallel to (010). It is coordinated by one $\text{M}(3)$ and two $\text{M}(1)$ cations, and is usually occupied by OH^- , F^- or O^{2-} . The mean interatomic distance between O(3) and its coordinating cations is significantly shorter in fluor-tremolite (2.042\AA vs 2.074\AA in hydroxyl tremolite). This can be explained by the smaller effective size of three-coordinated F.

The $T(1)-T(1)$ distances across the mirror plane are significantly smaller in fluor-tremolite (3.002\AA) than in hydroxyl tremolite (3.030\AA) and reflect the narrower $T(1)-\text{O}(7)-T(1)$ angle in fluor-tremolite (138.3° vs 139.3°). Papike *et al* (1969) located the proton in hydroxyl tremolite within the mirror plane at an angle of 94 degrees with respect to the octahedral strip. This location of the proton may explain the wider angle in hydroxyl tremolite as resulting from attraction between the proton and O(7), or possibly, as an antibonding repulsion between the proton and the two silicon atoms.

Effect of O(3) occupancy on the thermal stability of tremolite

As the occupancy of O(3) is the only chemical variable in the two tremolite structures, their differing thermal stabilities may be related either (1) to effects induced in the amphibole structure by the substitution of F for OH, or (2) to the instability of the OH in hydroxyl tremolite at high temperatures. Comparison of the hydroxyl and fluor-tremolite structures shows that the most significant difference is the smaller size of the octahedral layer in fluor-tremolite. The shorter Mg-F distances suggest stronger bonds, and an examination of the bond strengths reveals that the Mg-F bond is stronger than the Mg-O bond (105.5 kcal/mole vs 83 kcal/mole; *Handbook of Chemistry and Physics*, 51st edition). This difference in bond strengths may contribute to the higher thermal stability of fluor-tremolite.

Another important factor affecting the relative stabilities of hydroxyl and fluor-tremolite is the behavior at high temperatures of the OH in hydroxyl tremolite. Addison *et al* (1962) proposed a mechanism for the simultaneous oxidation and dehydroxylation of an Fe-bearing amphibole in oxidizing atmospheres. The mechanism involves the loss of a proton from a hydroxyl group with local charge balance being restored by the oxidation of an adjacent ferrous iron. Patterson and O'Connor (1966) in their infrared

investigations of the fibrous amphiboles crocidolite ($\text{Na}_2\text{Fe}_2^{3+}\text{Fe}_3^{2+}\text{Si}_8\text{O}_{22}(\text{OH})_2$), amosite ($(\text{MgFe}^{2+})_7\text{Si}_8\text{O}_{22}(\text{OH})_2$) and tremolite ($\text{Ca}_2\text{Mg}_5\text{Si}_8\text{O}_{22}(\text{OH})_2$) showed, for the two Fe-bearing amphiboles, that dehydroxylation in air is completed without decomposition and that their decomposition temperature approaches or equals that of the tremolite. When the two Fe-bearing amphiboles are heated in a vacuum, the temperature of dehydroxylation increases, the temperature of decomposition decreases by $\sim 200^\circ\text{C}$, and decomposition is simultaneous with or occurs in the latter stages of dehydroxylation. The lower temperature of decomposition may be attributed to the fact that charge balance cannot be maintained in a vacuum, once the protons are lost, because the Fe^{2+} is prevented from oxidizing. In tremolite, dehydroxylation and decomposition occur simultaneously, regardless of whether the sample is heated in air or in vacuum, and the dehydroxylation mechanism may be similar to that of the Fe-bearing amphiboles which were heated in a vacuum. Nevertheless loss of the proton in the tremolite probably results in extreme charge imbalance in the structure causing the amphibole to break down.

Conclusions

The substitution of F for OH in the tremolite structure reduces the size of the octahedral layer (by $\sim 0.1\text{--}0.2\text{\AA}$) and, accordingly, the a and b cell parameters. This reduction in size can be explained by the fact that three-coordinated fluorine is smaller than three-coordinated hydroxyl. The $T(2)$ -tetrahedron in both structures is larger ($\sim 1.632\text{\AA}$ vs 1.620\AA) and more distorted than the $T(1)$ -tetrahedron. Differences in the steric details of the tetrahedra in hydroxyl tremolite and fluor-tremolite can be explained in terms of differences in the octahedral layers. The larger $T(1)\text{--}O(7)\text{--}T(1)$ angle in hydroxyl tremolite has been attributed to attraction between $O(7)$ and the proton on OH and to antibonding repulsion between the two silicon atoms and the proton.

A comparison of the structures seems to indicate that there are no differences significant enough to stabilize the fluor-tremolite to considerably higher temperatures. The differences in the thermal stabilities of the two amphiboles must be related in part to the stronger Mg-F bonds and in part to the fact that loss of OH in hydroxyl tremolite destabilizes the structure, causing such an excessive charge imbalance that it breaks down.

TABLE 8. Mean Quadratic Elongation

	Hydroxyl tremolite	Fluor-tremolite
M(1) octahedron	1.0108	1.0142
M(2) octahedron	1.0073	1.0073
M(3) octahedron	1.0132	1.0149
T(1) tetrahedron	1.0033	1.0006
T(2) tetrahedron	1.0042	1.0043

Acknowledgments

We thank Professors F. D. Bloss, M. C. Gilbert, and P. H. Ribbe of VPI & SU, J. J. Papike and C. T. Prewitt of SUNY, and S. Ghose of the University of Washington for reading and constructively criticizing the manuscript. The Carnegie Institute of Washington, D.C., is acknowledged by the senior author for a predoctoral fellowship during the period January 1 through August 31, 1971. This study was undertaken with a program of research supported by the National Science Foundation Grant GU-3192.

References

- ADDISON, C. C., W. E. ADDISON, G. H. NEAL, AND J. H. SHARP (1962) Amphiboles. Part I. The oxidation of crocidolite. *J. Chem. Soc.* **1962**, 1468-1471.
- BARTELL, L. S., L. S. SU, AND HSIUKANG YOW (1970) Lengths of phosphorus-oxygen and sulfur-oxygen bonds. An extended Hückel molecular orbital examination of Cruickshank's $d_{\pi}\text{--}p_{\pi}$ picture. *Inorg. Chem.* **9**, 1903-1912.
- BASCH, H., A. VISTE, AND H. B. GRAY (1965) Valence orbital ionization potentials from atomic spectral data. *Theoret. Chim. Acta*, **3**, 458-464.
- BAUR, W. H. (1961) Distorted coordination polyhedra in heteropolar crystal structures and the electrostatic valence rule of Pauling. *Naturwissenschaften*, **48**, 549.
- (1970) Bond length variation and distorted coordination polyhedra in inorganic crystals. *Trans. Amer. Crystallogr. Ass.* **6**, 125-155.
- BOYD, F. R. (1959) Hydrothermal investigations of amphiboles, In P. H. Abelson, Ed., *Researches in Geochemistry, Vol. 1*, John Wiley and Sons, Inc., New York, pp. 377-396.
- BUSING, W. R., K. O. MARTIN, AND H. A. LEVY (1962) ORFLS, a Fortran crystallographic least-squares program. *U.S. Nat. Tech. Inform. Serv.* **ORNL-TM-305**.
- , ———, AND ——— (1964) ORFFE, A Fortran crystallographic function and error program. *U.S. Nat. Tech. Inform. Serv.* **ORNL-TM-306**.
- CLEMENTI, E., AND D. L. RAIMONDI (1963) Atomic screening constants from SCF functions. *J. Chem. Phys.* **38**, 2686-2689.
- COMEFORO, J. E., AND J. A. KOHN (1954) Synthetic asbestos investigations. I: Study of synthetic fluor-tremolite. *Amer. Mineral.* **39**, 537-548.
- DOYLE, R. A. AND P. S. TURNER (1968) Relativistic Hartree-Fock X-ray and electron scattering factors. *Acta Crystallogr.* **24A**, 390-397.
- ERNST, W. G. (1962) Synthesis, stability relations, and occurrence of riebeckite and riebeckite-arfvedsonite solid solutions. *J. Geol.* **70**, 689-736.

- GIBBS, G. V. (1969) Crystal structure of protoamphibole. *Mineral. Soc. Amer. Spec. Pap.* **2**, 101–109.
- , M. M. HAMIL, S. J. LOUISNATHAN, L. S. BARTELL, AND H. YOW (1972) Correlations between Si–O bond length, Si–O–Si angle, and bond overlap populations calculated using extended Hückel molecular orbital theory. *Amer. Mineral.* **57**, 1578–1613.
- , S. J. LOUISNATHAN, P. H. RIBBE, AND M. PHILLIPS (1973) Semi-empirical molecular orbital calculations for the atoms of the tetrahedral framework in anorthite, low albite, maximum microcline, and reedmergnerite. In, W. S. MacKenzie and J. Zussman, Eds., *Proc. N.A.T.O. Advanced Studies Institute on Feldspars*, Manchester University Press, Manchester.
- HAMILTON, W. C. (1965) Significance tests on the crystallographic *R*-factor. *Acta Crystallogr.* **18**, 502–510.
- HANSON, A. W. (1965) The crystal structure of the axulene, S-trinitrobenzene complex. *Acta Crystallogr.* **19**, 23–47.
- HOFFMAN, R. (1963) An extended Hückel theory. I. Hydrocarbons. *J. Chem. Phys.* **39**, 1397–1412.
- LOUISNATHAN, S. J., AND G. V. GIBBS (1972) The effect of tetrahedral angles on Si–O bond overlap populations for isolated tetrahedra. *Amer. Mineral.* **57**, 1614–1642.
- PANT, A. K., AND D. W. J. CRUICKSHANK (1967) A reconsideration of the structure of datolite, $\text{CaBSiO}_4(\text{OH})$. *Z. Kristallogr.* **125**, 286–297.
- PAPIKE, J. J., M. ROSS, AND J. R. CLARK (1969) Crystal-chemical characterization of clinoamphiboles based on five new structure refinements. *Mineral. Soc. Amer. Spec. Pap.* **2**, 117–136.
- PATTERSON, J. H., AND D. J. O'CONNOR (1966) Chemical studies of amphibole asbestos. I. Structural changes of heat-treated crocidolite, amosite, and tremolite from infrared absorption studies. *Aust. J. Chem.* **19**, 1155–1164.
- PAULING, L. (1961) *The Nature of the Chemical Bond*. Cornell University Press, Ithaca, N.Y., 3rd ed.
- RIBBE, P. H., AND G. V. GIBBS (1971) Crystal structures of the humite minerals. III. Mg/Fe ordering in humite and its bearing on other ferromagnesian silicates. *Amer. Mineral.* **56**, 1155–1173.
- ROBINSON, K., G. V. GIBBS, AND P. H. RIBBE (1971) Quadratic elongation: A quantitative measure of distortion in coordination polyhedra. *Science*, **172**, 567–570.
- SMITH, J. V. (1954) Re-examination of the crystal structure of melilite. *Amer. Mineral.* **38**, 643–661.
- TROLL, G., AND M. C. GILBERT (1972) Fluorine-hydroxyl substitution in tremolite. *Amer. Mineral.* **57**, 1386–1403.
- WARREN, B. E. (1929) The structure of tremolite, $\text{H}_2\text{Ca}_2\text{Mg}_5(\text{SiO}_3)_8$. *Z. Kristallogr.* **72**, 42–57.
- WOLFSBERG, M., AND L. HELMHOLZ (1952) The spectra and electronic structure of the tetrahedral ions MnO_4^- , CrO_4^- , and ClO_4^- . *J. Chem. Phys.* **20**, 837–843.
- ZUSSMAN, J. (1959) A re-examination of the structure of tremolite. *Acta Crystallogr.* **12**, 309–312.

Manuscript received, January 16, 1973; accepted for publication, April 17, 1973.